The Shell evolution of the hydrocenidae of Malaysian Borneo

Bin Khalik, M.Z.

Chapter 4

Morphological parallelism of sympatric cave-dwelling microsnails of the genus *Georissa* at Mount Silabur, Borneo (Gastropoda, Neritimorpha, Hydrocenidae).

Mohd Zacaery Khalik[1,2,3], Esra Bozkurt[1] and Menno Schilthuizen[1,2,4]

Published chapter

Khalik, M. Z., Bozkurt, E., and Schilthuizen, M. (2019). Morphological parallelism of sympatric cave‐dwelling microsnails of the genus *Georissa* at Mount Silabur, Borneo (Gastropoda, Neritimorpha, Hydrocenidae). *Journal of Zoological Systematics and Evolutionary Research*.

1 Naturalis Biodiversity Center, Darwinweg 2, 2333 CR Leiden, The Netherlands.
2 Institute of Biology Leiden, Faculty of Science, Leiden University, Sylviusweg 72, 2333 BE Leiden, The Netherlands.
3 Faculty of Resource Science and Technology, Universiti Malaysia Sarawak, 94300 Kota Samarahan, Sarawak, Malaysia.
4 Institute for Tropical Biology and Conservation, Universiti Malaysia Sabah, Jalan UMS, 88400 Kota Kinabalu, Sabah, Malaysia.

Abstract

Parallel evolution in phenotype may result when closely related taxa are adapting in the face of similar ecological pressures. Here, we discuss possible parallelism in shell morphology in the context of the microgeographic phylogeography of two conchologically distinct sympatric hydrocenid snails inhabiting a limestone outcrop and its cave system, *Georissa pyrrhoderma* and *Georissa silaburensis*, respectively, at Mount Silabur in Sarawak, Malaysian Borneo. Our results show a certain degree of morphological parallelism between *G. silaburensis* and a third, possibly new, cryptic *Georissa* species within the same cave that diverged from its above-ground sister species, *G. pyrrhoderma*. We found that both sympatric cave species have shifted from a more sculptured, conical shell towards a broader, less sculptured form.

Introduction

Convergent evolution and parallelism have been a subject of studies related to genotype and phenotype evolution in a wide range of taxa, including mammals (Madsen et al., 2001), reptiles (Revell et al., 2007; Stayton, 2006), birds (Fain and Houde, 2004; Grenier and Greenberg, 2005), and fishes (Rüber and Adams, 2001; Hulsey et al., 2008; Qi et al., 2012). Convergence and parallelism are the outcomes of evolutionary processes in which different species independently converge towards similar, adaptive phenotypes. Usually, the term convergence is reserved for superficially similar but non-homologous traits that evolve in distantly related taxa, whereas parallelism refers to similar morphologies involving homologous structures in more closely related taxa (Alejandrino et al., 2011). To address and understand the processes involved, researchers often investigate the evolutionary patterns in organisms that respond to similar environmental changes and concomitant selection (Houle, 1991; Rundle and Nosil, 2005). Using molecular-phylogenetic reconstruction, detailed phenotype changes in multiple species make further analysis and interpretation of selected taxa possible, allowing an understanding of their evolutionary diversification.

Studies on convergent evolution and morphological parallelism have demonstrated that similar phenotypic traits often result when taxa are facing similar ecological pressures (in, e.g., microhabitat, climate, diet, predator

pressure, etc.). For example, Kaeuffer et al. (2010) studied the intraspecific phenotypic diversity of threespine stickleback fish from different aquatic environments and concluded that morphological characters such as body depth and gill raker numbers show strong morphological convergence. In a different study, Lindgren et al. (2012) investigated the interspecific morphological divergence and convergence of Cephalopoda; they found convergent evolution in cephalopods of similar habitat types, even in distantly related taxa. For example, taxa with an autogenic photophore were always associated with a pelagic habitat, while the benthic habitat harboured taxa characterised by the presence of corneas and accessory nidamental glands. Both these studies employed detailed study of morphological characters and molecular data to reconstruct the evolutionary relationship among different taxa, and interpreted these in the context of the ecological factors that drive the evolution of similar morphological traits.

Rock-dwelling land snails of Southeast Asia often show high allopatric and sympatric diversity with many species endemic to small geographic regions (Liew et al., 2014; Rundell, 2008; Tongkerd et al., 2004), especially species inhabiting karstic environments. This can sometimes make it difficult to decide on the taxonomic status of similar-shelled forms. Usually, these are considered as conspecific based on shared shell characters (**Chapters 2 and 3**; Foon and Liew, 2017; Liew et al. 2014; Thompson and Dance, 1983; Vermeulen et al., 2015). Furthermore, phylogenetic analyses often reveal that the detailed conchology follows the patterns of phylogenetic relatedness (**Chapters 2 and 3**; Schilthuizen et al., 2005; Schilthuizen et al., 2012). Nonetheless, possible cases of morphological parallelism due to ecological similarity may be overlooked.

Shell variation in a single land snail species has often been shown to be correlated with variation in habitat (Baur, 1988; Cameron and Cook, 1989; Chiba, 2004; Chiu et al., 2002; Goodfriend, 1986; Haase and Misof, 2009). This means that different ecological systems provide different selective pressures and induce adaptive changes in a population's morphological characters. Eventually, this may lead to speciation (Chazot et al., 2016; Danowitz et al., 2015; Price et al., 2003). Hirano et al. (2014) recently showed that a molecular phylogenetic and morphological analysis revealed parallelism in multiple lineages of camaenid land snails. They found that an angularity of

the shell periphery appeared at least seven times in the phylogeny. Although their study focused on the discordance between shell morphology and molecular phylogenetics which could impinge on taxonomic classification, their study also provides an important example of parallelism.

Here, we investigate microgeographic patterns of molecular phylogeny and conchometric characters of sympatric species of Hydrocenidae Troschel, 1856 (microsnails of the genus *Georissa* Blanford, 1864) inhabiting the above and below-ground areas of the limestone hill Mount Silabur in Sarawak, Malaysian Borneo. Due to the common occurrence and high abundance of hydrocenids in the region, we were able to conduct a systematic sampling design to understand the evolutionary patterns, specifically shell character changes inferred by molecular phylogeny. The above-ground limestone outcrop and the below-ground cave systems are two microhabitats with extremely different environmental conditions. In general, the below-ground conditions are darker, with smaller temperature and humidity fluctuations, a less complex foodweb, and lower energy availability (Barr, 1967; Poulson and White, 1969).

Thus, we attempt to reconstruct the phylogenetic relationships among three sympatric hydrocenid forms of the genus *Georissa*, originating from 19 different populations sampled from the limestone outcrop and cave. Two sympatric *Georissa* species were previously known to occur at the Mount Silabur limestone hill, namely *G. pyrrhoderma* Thompson and Dance, 1983, inhabiting the limestone outcrops surrounding the hill, and *G. silaburensis* Khalik, Hendriks, Vermeulen, and Schilthuizen, 2018, inhabiting the cave interior (**Chapter 2**). Similarly to what was found for the troglobitic species *G. filiasaulae* Haase and Schilthuizen, 2007 from Sepulut, Sabah), the cave-inhabiting *G. silaburensis* has a relatively large, broad shell, reduced shell sculpture, and is less pigmented compared to the sympatric epigean species inhabiting the outcrops, typical (and variant) *G. pyrrhoderma* (**Figure 4.3A**). Based on shell morphology, we found a third form, inhabiting the cave environment, *Georissa* "sp. Silabur" (**Figure 4.3C**), of which the shell shape is similar to the typical *G. silaburensis* whereas the scale characters are similar to the typical *G. pyrrhoderma*.

In this study we therefore subject this complex of three shell forms to a morphological and molecular analysis to reveal patterns of phylogenetic relatedness among them, and offer a scenario for their evolution.

Material and Methods

Study site

The sampling was conducted at an isolated limestone hill, Mount Silabur, Serian, Sarawak, Malaysian Borneo (00°57.407'N, 110°30.276'E). Mount Silabur is approximately 350 metres high and measures roughly 500 by 300 metres. The cave entrance is about 150 metres from the foot of the hill. The cave itself consists of a main chamber connecting the opposite sides of the hill. There are multiple high chambers (Wilford, 1964) that we excluded from our sampling for safety reasons. Our first fieldwork was on the 3rd of March 2017, when random sampling was carried out at two locations at the limestone outcrops and one location in the cave. The second sampling took place on the 16th of April 2017, when we conducted systematic sampling and sketched a map of the cave system in which we also indicated the location of the plots (**Figure 4.1**). Populations of hydrocenids were collected at 19 different plots surrounding the outcrops and inside of the cave.

Sampling method

The sampling locations consist of 13 plots (plots SIE1-SIE6, SIO1-SIO6, and SO3) outside the cave and six plots (plots SIG1-SIG6) inside the cave of Mount Silabur. Apart from these plots, we also encountered 10 sites where no hydrocenids were found (**Figure 4.1**). The plots surrounding the hill were located approximately 5-10 metres away from the established trails. We generally selected humid, shaded limestone rocks covered with vegetation. The plots inside of the cave were mainly the vertical limestone walls of the main chamber. The distance between two plots was set to be at least 20 metres. We spent about 20 minutes at each (approximately circular) plot with two collectors searching on the limestone rocks and walls, vegetation and the surrounding areas, within an approximately five metres diameter. The collected living materials were directly stored in ~96% ethanol.

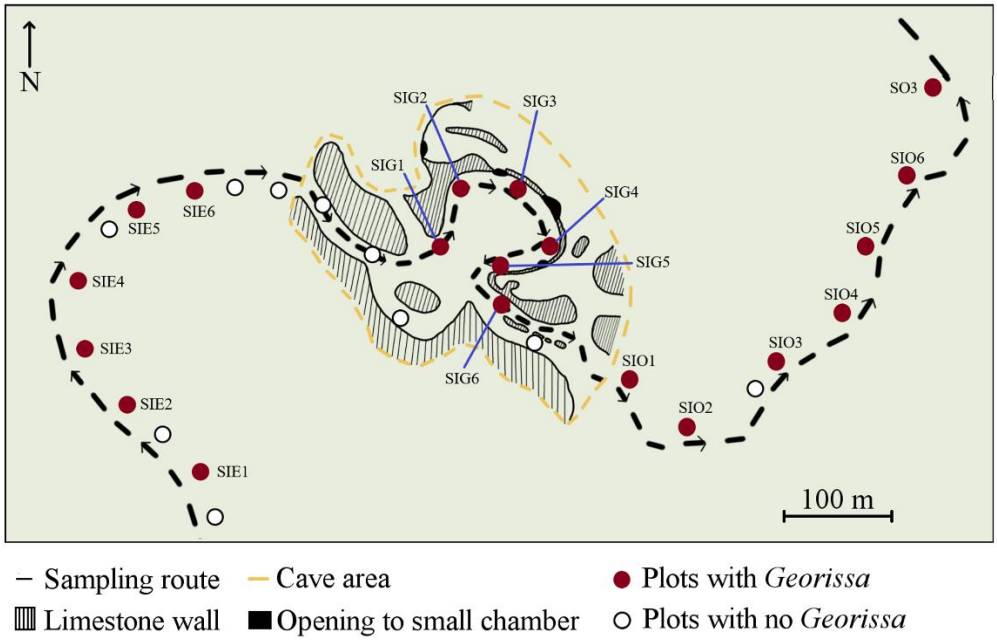

Figure 4.1 Sampling transect and plots at Mount Silabur outcrops and cave environments. Abbreviation used for each sampling plot during the fieldwork; S/SI = Silabur; E = before cave; G = inside cave; O = after cave.

Shell measurement and scanning electron microscope (SEM)

A composite 2D image of each individual shell was obtained from the focus-stacked images captured with a Zeiss SteREO Discovery.V20 stereo-microscope. The images were taken at 40× magnification and 100 µm layer thickness at constant light intensity. We used the apertural view of the individual shell to measure the shell height (SH), shell width (SW), aperture height (AH), and aperture width (AW). Details on the shell measurements are in Supporting Information (Table S1).

For each shell form we determined the characters based on the shell shape and sculpture patterns. We performed scanning electron microscopy (SEM) using a JEOL JSM-6480LV to obtain detailed views of the sculptural patterns. All hydrocenid shells were grouped into shell form categories based on their detailed shell shape and surface characters.

A total of 274 adult shells of hydrocenids from all sampling plots were used in the morphometric analysis. We also included specimens of the closest relative of *G. silaburensis*, viz. *G. bauensis* Khalik, Hendriks, Vermeulen, and Schilthuizen, 2018 (17 adult shells) from Wind Cave Nature Reserve (WNCR), Bau, Sarawak (approximately 50 km from Mount Silabur). We made scatterplots of measured characters in RStudio (RStudio Team, 2016) to visualise the morphological variation of the measured adult shell forms (Supporting Information Table S1).

DNA extraction and amplification

Genomic DNA of the snails was extracted with Qiagen DNeasy Blood and Tissue kit using the manufacturer's protocol. Prior to the extraction, the shells were crushed and removed (partially). The entire soft tissue was used in the extraction. Three partial DNA regions were amplified, *16S* ribosomal RNA ("*16S*") and *cytochrome c oxidase subunit I* ("*COI"*) for mitochondrial markers, and *28S* ribosomal RNA ("*28S*") for a nuclear marker. A fragment of *16S* region was amplified using primer pair LR-J-12887 5'-CCGGTCTGAACTCAGATCACGT-3' (forward) and LR-N-13398 5'-CGCCTGTTTAACAAAAAACAT-3' (reverse) (Schilthuizen et al., 2005). For the *COI* region, we used primer pair LCO1490 5'-GGTCAACAAATCATAAAGATATTGG-3' (forward) and HCO2198 5'-TAAACTTCAGGGTGACCAAAAAATCA-3' (reverse) (Folmer et al., 1994) in the amplification process. We also amplified a partial *28S* DNA nuclear region using primer set D23F 5'-GAGAGTTCAAGAGTACGTG-3' (forward) and D6R 5'-CCAGCTATCCTGAGGGAAACTTCG-3' (reverse) (Park and Ó Foighil, 2000).

PCR were performed in 25.0 µL reaction volume containing 1.0 µL undiluted DNA template, which consist of: 12.5-17.0 µL ultrapure water milli-Q, 5.0 µL Qiagen Q-solution (only for *28S* amplification), 2.5 µL Qiagen PCR chlorine buffer 10×, 1.0-2.5 µL Qiagen $MgCl_2$ 25.0 mM, 0.25-1.0 µL Promega BSA 100 mM (only for *16S* and *COI* amplification), 1.0 µL forward primer 10 pmol/ µL, 1.0 µL reverse primer 10 pmol/ µL, 0.5 µL dNTPs 2.5 mM, and 0.25 µL Qiagen Taq 5.0 U/ µL. The PCR program started with initial denaturation at 95°C for 5 min, followed by 36-40 cycles of denaturation at 95°C for 15-45 s, annealing at 50-55°C for 30-40 s, extension at 72°C for 1-2 min, and a final

extension at 72°C for 5-10 min. DNA amplifications were performed on a BIO-RAD C1000 Touch^{TM} Thermal Cycler. The PCR products were then Sanger sequenced in both directions at BaseClear B.V. (Leiden, The Netherlands). The amplification length of each *16S*, *COI*, and *28S* genes are 530-532, 708-710, and 830-834 bp, respectively, including primers of both directions. The newly obtained sequences were assembled using the *de novo* Geneious 10.2.3 assembler, manually checked and edited, and primer sequences at both ends were trimmed. The resulted sequence lengths of each *16S*, *COI*, and *28S* genes are 481-486, 602, and 700-788 bp, respectively. The new sequences were deposited in GenBank (https://www.ncbi.nlm.nih.gov/WebSub/) and BOLD (http://boldsystems.org/). Details of the specimens used in this study are listed in Supporting Information (Table S2). The accession number for *16S*, *CO1* and *28S* genes are MK775735-MK775820, MK811455-MK811541 and MK775829-MK775944, respectively.

Phylogenetic analyses

We used *16S* and *COI* mtDNA sequences of other Bornean *Georissa* species, namely *G. gomantonensis*, *G. hosei*, *G. sepulutensis*, *G. kinabatanganensis*, and *G. bauensis*, and the outgroups *Bathynerita naticoidea*, *Nerita maxima* and *Nerita patula*. These sequences were obtained from our previous studies, Aktipis and Giribet (2010), and Frey and Vermeij (2008), respectively. Our previous study (see **Chapters 2 and 3**) have shown that *G. bauensis* is sister to *G. silaburensis*, while *G. sepulutensis* and *G. kinabatanganensis* are sister to *G. pyrrhoderma*. For these particular reasons, we included these three taxa in our current study. The sequences were aligned using default parameters of MUSCLE (Edgar, 2004). The alignment of *COI* mtDNA was set to invertebrate mitochondrial genetic code at the second reading frame.

We performed a maximum likelihood (ML) analysis using the concatenated *16S* and *COI* mitochondrial and nuclear *28S* genes, with 5000 rapid bootstrap replicates (Hoang et al., 2017) using IQ-TREE 1.6.3 (Nguyen et al., 2015). The best fit nucleotide substitution model for each gene was determined using ModelFinder (Kalyaanamoorthy et al., 2017) based on the corrected Akaike Information Criterion (AICc). The best fit nucleotide substitution models for *28S*, *16S*, and *COI* were TIM3+F+G4, HKY+F+G4, and TIM+F+G4, respectively. In addition, we also conducted separate ML analyses of

mitochondrial and nuclear genes. Bayesian inference (BI) was performed with MrBayes 3.2.6 (Huelsenbeck and Ronquist, 2001) using the following MCMC settings: GTR+G+I nucleotide substitution model; 1,100,000 generations; tree subsampling for every 200 generation; a burn-in of 100,000; 4 heated chains with heated chain temperature at 0.2.

Haplotype network and genetic divergence

A total of 112 *COI* sequences of hydrocenids including those of *G. silaburensis* and *G. pyrrhoderma* from **Chapter 2** were used for the haplotype study. The sequences were aligned using MUSCLE (Edgar, 2004), and both ends were trimmed to give a set of 603 bp sequences, with no gaps. The haplotype groups were determined with DNAsp ver. 6.12.01 (Rozas et al., 2017) and the median joining network was calculated and constructed in Network ver. 5.0.1.1 (Fluxus Technology Ltd, Kiel, Germany).

To determine the genetic divergence among the sympatric conchologically distinguishable forms, we conducted genetic distance analysis in MEGA v. 7.0.26 (Kumar et al., 2016) based on the same *COI* sequence alignment as used in the phylogenetic analysis above. We computed pairwise genetic distances between each pair of individuals and between different shell forms based on the Kimura 2-parameter nucleotide substitution model, selecting the transition + transversion, uniform rates among sites, and 1000 bootstraps for variance estimation.

Results

Microhabitats and shell characteristics

Our fieldwork resulted in a thorough population sampling of *Georissa* at Silabur. Initially, we made 29 plots comprising 10 plots in the cave and 19 above-surface plots at the limestone outcrops. We were able to find and collect *Georissa* at six plots in the cave and 13 plots at the outcrops. Sampling started at the foot of the hill, plot SIE1 (00°57.407'N, 110°30.276'E) at approximately 50 metres a.s.l., which was the lowest sampling point. The highest sampling plot was SIO2 (00°57.388'N, 110°30.161'E) at approximately 168 metres a.s.l. Our random survey of the higher levels of the hill failed to yield any living hydrocenids. This may have been due to the fact that the upper part of hill is

directly exposed to sunlight and consists of dry limestone rocks, which might not be suitable for these minute land snails. Examples of different microhabitats where we did encounter *Georissa* are shown in **Figure 4.2**.

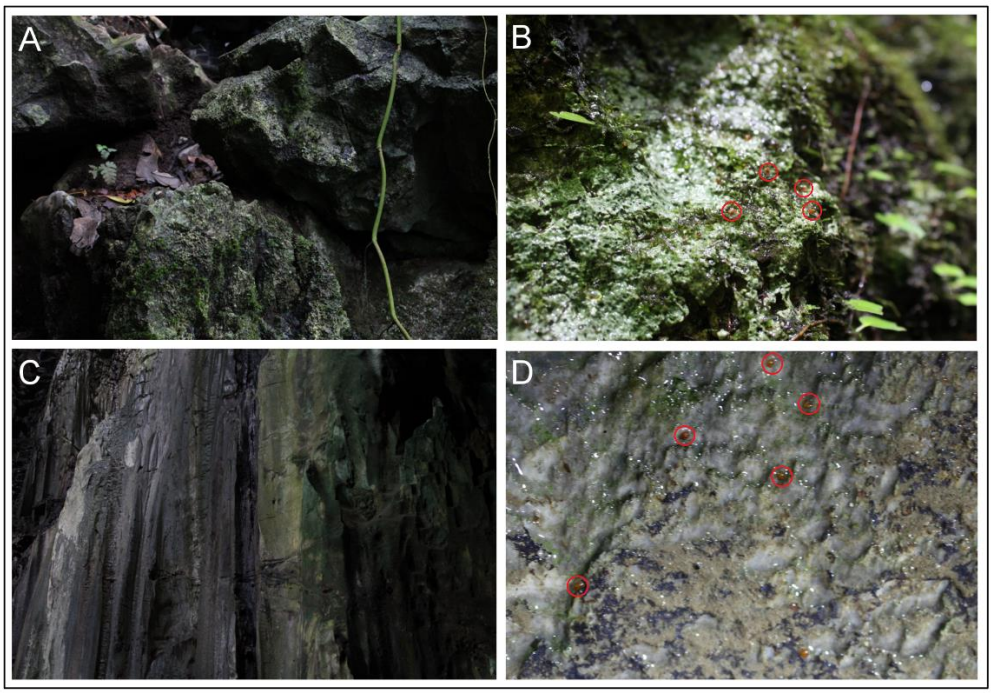

Figure 4.2 An overview of the different microhabitats of the studied hydrocenids. **A** Wet and shaded limestone rocks covered with lichen, a microhabitat of *Georissa* at the outcrops. **B** Close up image of the substrate showing *Georissa* foraging on the rock. **C** Vertical limestone cave wall with water slowly flowing from the cave ceiling. **D** Close up image of the cave wall showing *Georissa* foraging on the calcareous substrate. *Georissa* can be observed in **B** and **D**, which are minute, orange/red shells (circled in red).

During our morphological assessment of the hydrocenid shell, we were able to determine the morphological variation in each shell form. Qualitatively different sets of shell forms and their variation are shown in **Figure 4.3** and explained in **Table 4.1**.

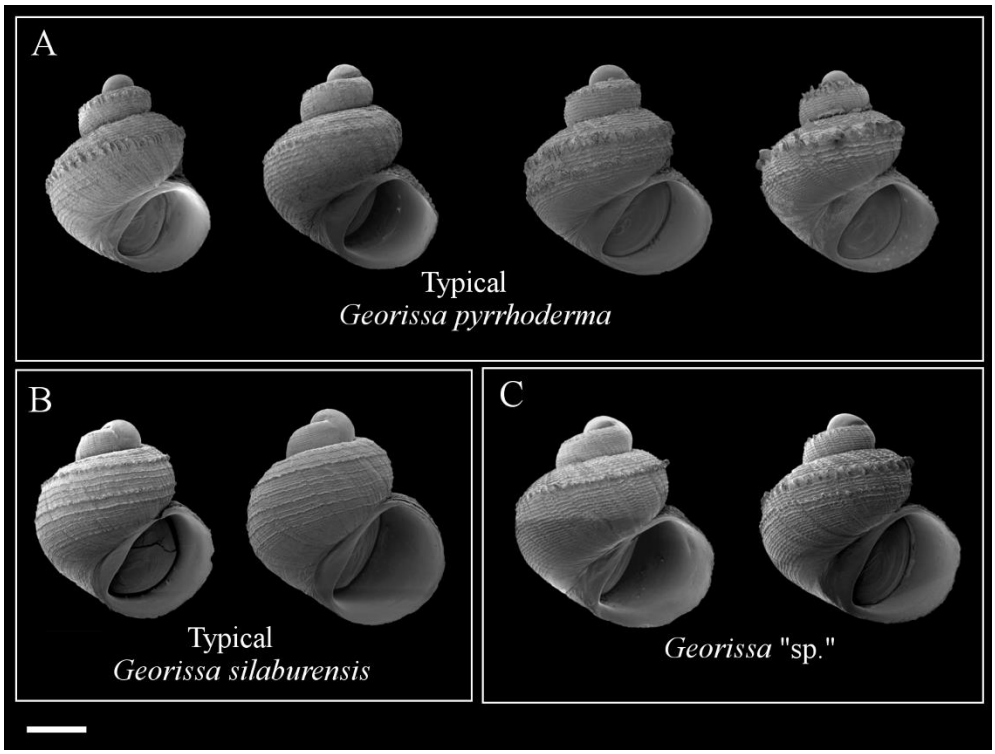

Figure 4.3 Scanning electron microscopy (SEM) images of detailed sculptural patterns of different forms of hydrocenids and their sculptural variation from Mount Silabur. **A** Typical *G. pyrrhoderma*. **B** Typical *G. silaburensis*. **C**. *Georissa* "sp. Silabur". See **Table 4.1** for explanations. Scale bar = 500 μm.

Table 4.1 Main characters and microhabitat of different forms of *Georissa*.

Shell forms	Microhabitat	Shell shape	Scales	Scale series
Typical *G. pyrrhoderma*	Outside of the cave	More conical	Wide and/or minute; reduced and/or raised	One or two
Typical *G. silaburensis*	Cave	More globular	Minute and reduced	Multiple
Georissa "sp. Silabur"	Cave	More globular	Minute and/or wide; reduced and/or raised	One or two

We made two shell measurement plots of hydrocenids from Mount Silabur, including *G. bauensis* from WNCR (**Figure 4.4**). The plots show that, in the cave, shell width is always greater with reference to shell height compared to the above-ground sister species of relatively similar shell height. As a result, a more globular shell shape is observed in the cave-dwelling species. Similar shape changes in general shell form and aperture appear when each surface-dwelling form is compared with the respective cave-dwelling sister form,

although the differences are stronger for the pair *G. bauensis* vs. *G. silaburensis* than for *G. pyrrhoderma* vs. *Georissa* "sp. Silabur"

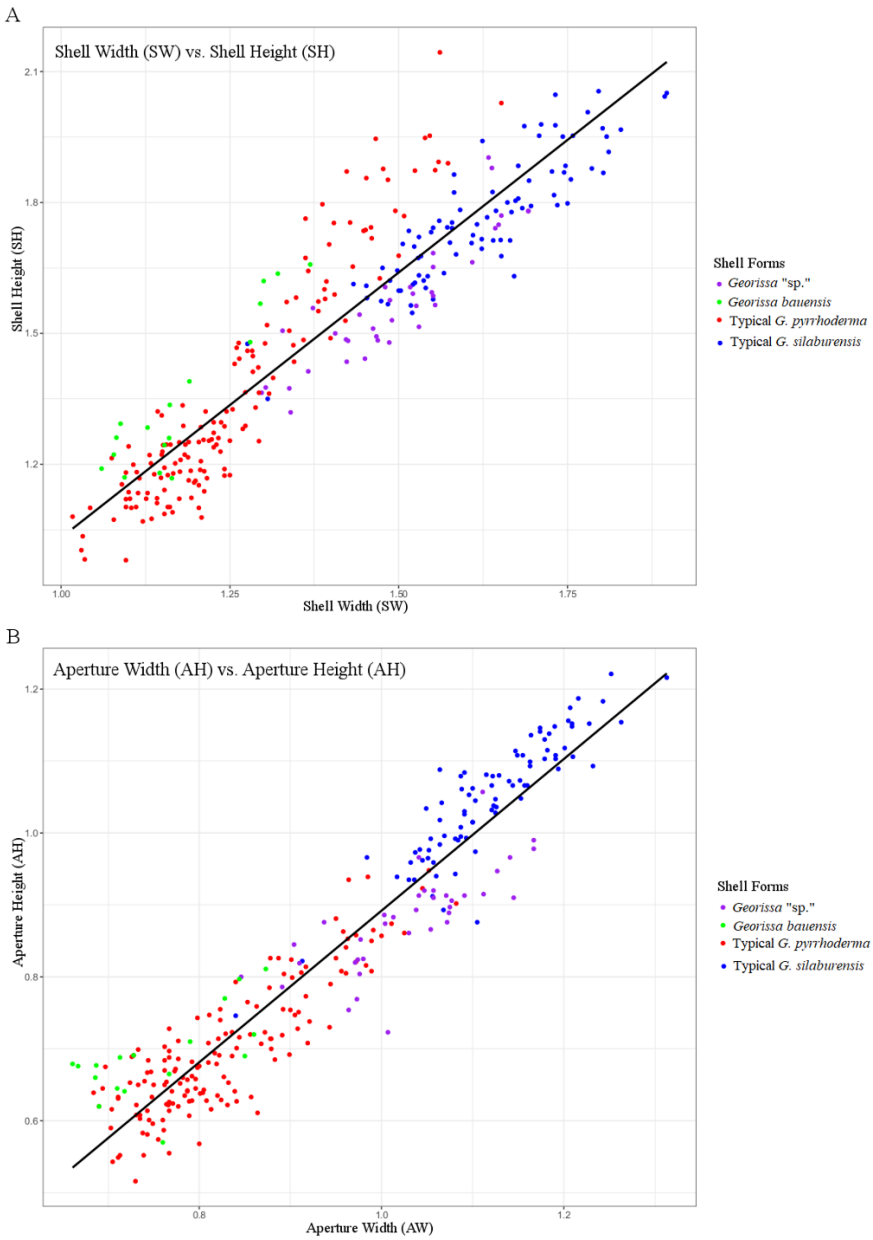

Figure 4.4 Shell measurement plots of a total 274 adult shells of different hydrocenid shell forms from Mount Silabur, including 17 adult shells of *G. bauensis* from WCNR. **A** Shell width vs. shell height. **B** Aperture width vs. aperture height.

Phylogenetic analyses

The maximum likelihood (ML) and Bayesian inference (BI) phylogenetic analyses result in slightly different tree topologies (**Figure 4.5 and 4.6**). Nonetheless, the results suggest that typical *G. silaburensis* and cryptic *Georissa* "sp. Silabur", which inhabit the cave environment are unrelated, despite their very similar (but not identical, see **Figures 4.3, 4.4a and 4.4b**) shell morphology and quantification. Typical *G. pyrrhoderma*, which inhabits the external part of the limestone outcrops is the sister species of *G. sepulutensis* and *G. kinabatanganensis* from Sabah, and paraphyletic with respect to *Georissa* "sp. Silabur".

Overall, we find the sympatric hydrocenids are divided into two major lineages, with typical *G. silaburensis* closely related to *G. bauensis* from WNCR, which is approximately 50 km away, and, typical *G. pyrrhoderma* and *Georissa* "sp. Silabur" phylogenetically close to *G. sepulutensis* and *G. kinabatanganensis* from Sabah, despite their geographical distance.

The ML cladogram of mitochondrial genes (Supporting Information Figure S2) shows a similar topology to the phylogenetic analyses (**Figures 4.5 and 4.6**). Additionally, we find the ML cladogram of the *28S* gene (Supporting Information Figure S3) is also in concordance with the ML and BI trees, which might indicate hybridisation between below-ground *Georissa* "sp. Silabur" and above-ground *G. pyrrhoderma*. Neither in the mitochondrial nor in the nuclear tree do we see any indication of introgression between the sympatric cave species (*G. silaburensis* and *Georissa* "sp. Silabur"), although they were found next to each other in at least three different plots, namely, SIG1, SIG3, and SIG5.

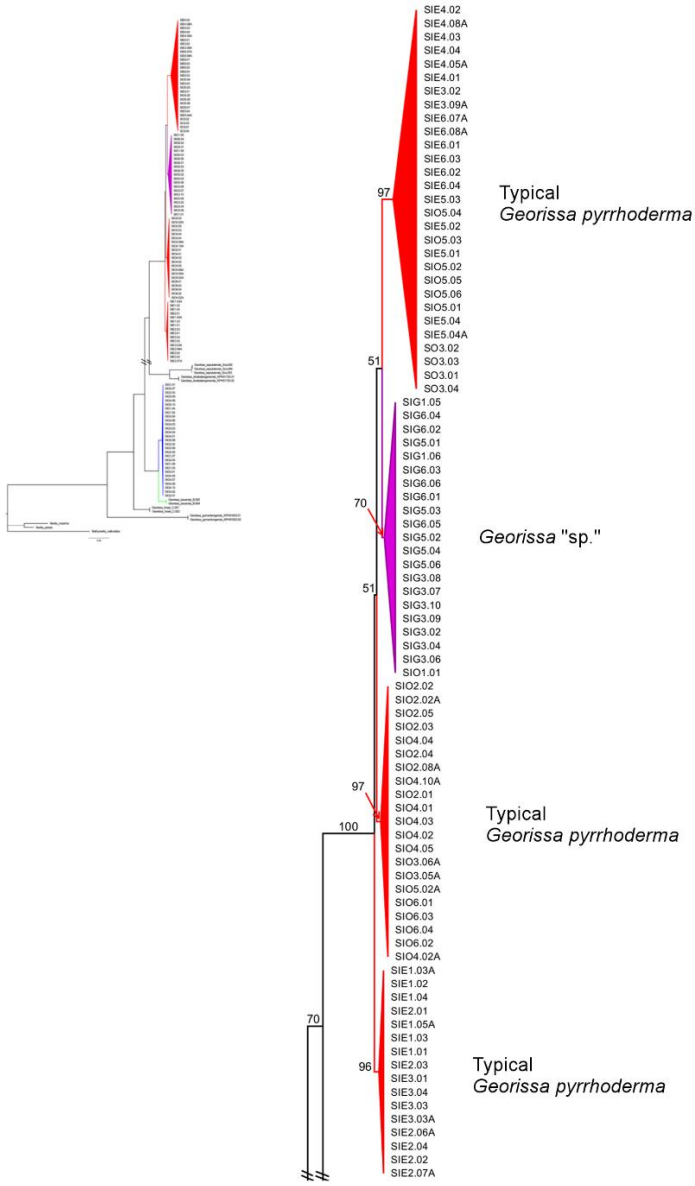

Figure 4.5 Maximum likelihood tree inferred by partitioned data of partial *16S* and *COI* mtDNA, and *28S* nDNA. The analysis was conducted with ultrafast bootstrapping (5000 replicates) with the respective nucleotide substitution models for each gene enforced in IQ-TREE 1.6.3. The tree consists of 127 individuals of Bornean hydrocenids, including *G. gomantonensis*, *G. hosei*, *G. bauensis*, *G. kinabatanganensis* and *G. sepulutensis* from Malaysian Borneo, with three outgroups taxa, namely, *Bathynerita naticoidea*, *Nerita patula* and *Nerita maxima*. Different colors of the clades indicate different form of hydrocenids (blue = typical *G. silaburensis*; red = typical *G. pyrrhoderma*; purple = *Georissa* "sp. Silabur"; green = *G. bauensis*).

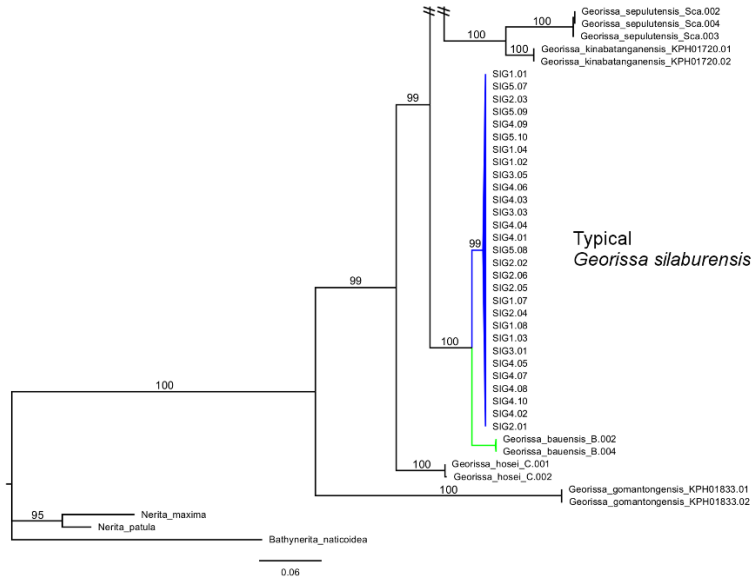

Figure 4.5 *Cont…*

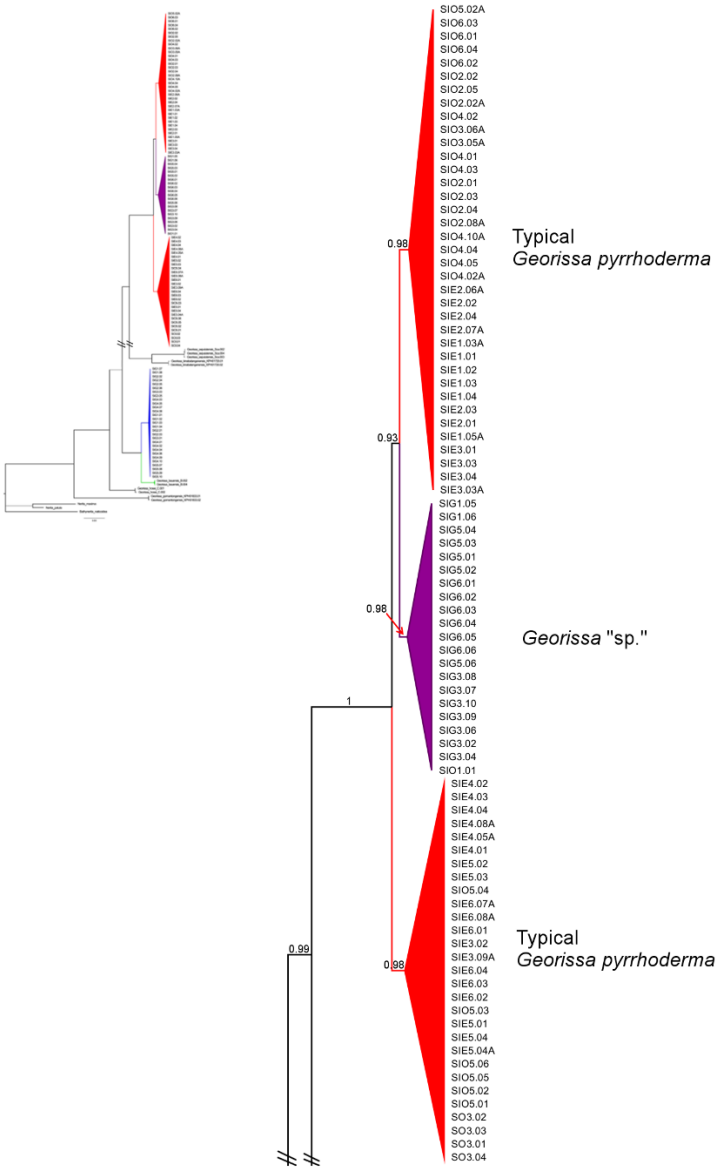

Figure 4.6 Bayesian inference tree inferred by concatenated sequence alignments of partial *16S* and *COI* mtDNA, and partial *28S* nDNA. The analysis consists of 127 individuals of Bornean hydrocenids, including *G. gomantonensis*, *G. hosei*, *G. bauensis*, *G. kinabatanganensis* and *G. sepulutensis* from Malaysian Borneo, with three outgroups taxa, namely, *Bathynerita naticoidea*, *Nerita patula* and *Nerita maxima*. Different colors of the clades indicate different form of hydrocenids (blue = typical *G. silaburensis*; red = typical *G. pyrrhoderma*; purple = *Georissa* "sp. Silabur"; green = *G. bauensis*).

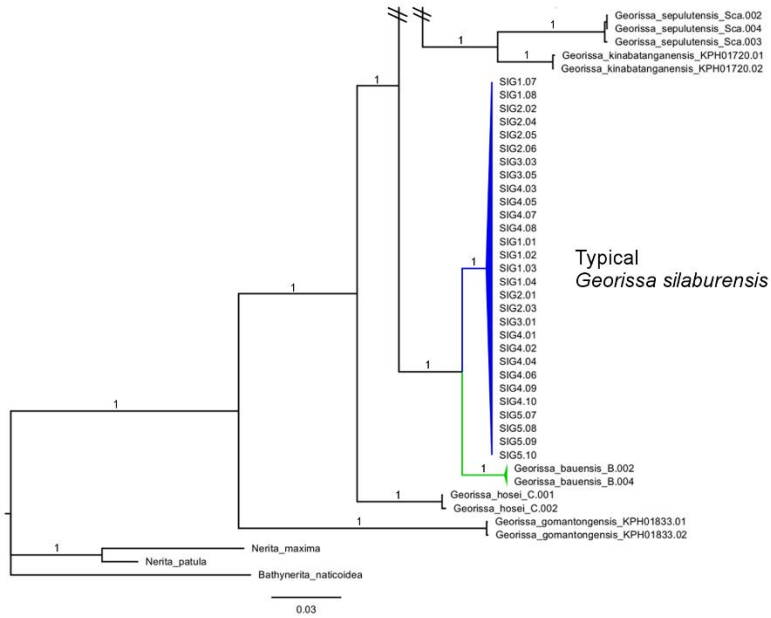

Figure 4.6 *Cont…*

Haplotype and genetic divergence

Sequence analysis of the partial *COI* gene resulted in a total of 32 unique haplotypes, with no insertions or deletions, differing only in base substitutions. From the median joining haplotype network (**Figure 4.7**), we are able to group the haplotypes into four major lineages, namely, H1 to H4, H17 to H28, H29 to H32, and H5 to H16, as the first, second, third and fourth lineages, respectively.

The haplotype network is consistent with our phylogenetic analyses, where organisms of different shell shape and size are grouped together in one clade. The shell form of typical *G. pyrrhoderma*, which is paraphyletic with respect to *Georissa* "sp. Silabur" in the phylogenetic trees, is divided into two major lineages in the haplotype study.

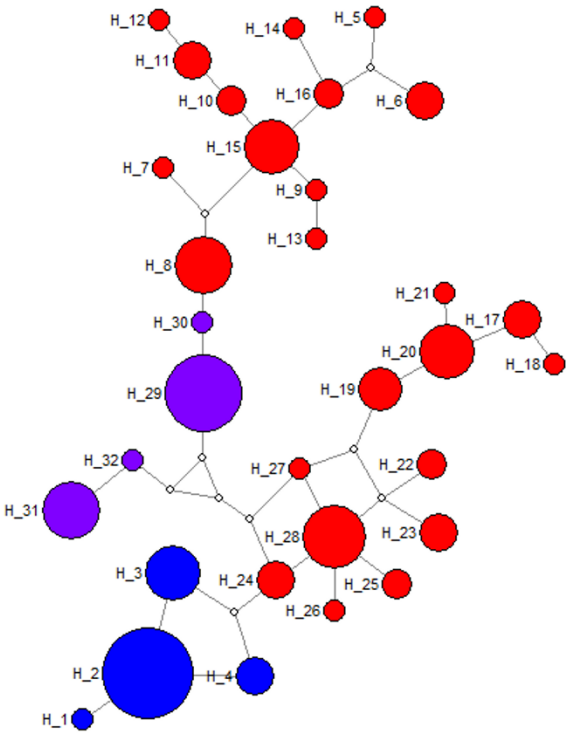

Figure 4.7 Median-joining haplotype network of 112 individuals of three major shell forms of *Georissa* of Mount Silabur based on *COI* mtDNA. Each haplotype is represented by a circle which is proportionate to the number of individuals bearing this haplotype. The colors represent different shell forms, namely, typical *G. silaburensis* (four haplotypes, blue), typical *G. pyrrhoderma* (24 haplotypes, red), and *Georissa* "sp. Silabur" (four haplotypes, purple). Details of the haplotype group of each individual are included in Supporting Information (Table S3).

COI genetic divergence

Our phylogenetic reconstructions and haplotype network have shown significant molecular divergences among all hydrocenid forms at Mount Silabur. Despite the similarity in morphological forms, the *COI* genetic divergences between sympatric cave species are high (distance of typical *G. silaburensis* to *Georissa* "sp. Silabur" = 13%), as shown in **Table 4.2**. The divergences between typical *G. silaburensis* (from the cave) to all other forms are 13% or more, whereas between typical *G. pyrrhoderma* (above-ground species) and *Georissa* "sp. Silabur" is lower (distance of *G. pyrrhoderma* to *Georissa* "sp. Silabur" = 5%).

Table 4.2 Genetic divergence of *COI* mtDNA between sympatric hydrocenids of Mount Silabur.

	Within group divergence	Number of specimens	Typical *G. silaburensis*	*Georissa* "sp. Silabur"
Typical *G. silaburensis*	1.13×10^{-3}	29		
Georissa "sp. Silabur"	1.40×10^{-2}	21	0.13	
Typical *G. pyrrhoderma*	4.71×10^{-2}	66	0.14	0.05

Discussion

Our results on phylogenetic analyses inferred by mitochondrial and nuclear genes show clear separation between each sympatric taxon and between each shell form (**Figures 4.5 and 4.6**). A combination of conchometric and phylogenetic analysis has provided a clear distinction among sympatric taxa, typical *G. silaburensis*, *G.* "sp. Silabur", and *G. pyrrhoderma*. Moreover, the phylogenetic analyses (**Figures 4.5 and 4.6**) indicate reproductive isolation between two morphologically very similar hydrocenid forms (typical *G. silaburensis* and *Georissa* "sp. Silabur") inhabiting the cave habitat. Additionally, *G. silaburensis* and *G.* "sp. Silabur" populations inside the cave habitat are completely mix. Based on our phylogenetic analysis, it shows population structuring between these two hydrocenid forms. The inferred phylogenies therefore provide evidence of parallelism in the shell size and shape of taxa of different lineages that independently have invaded the same cave habitat. In this case, we find a broader and more globular shell form with reduced sculpture in the troglobitic taxa, having evolved from the presumed ancestral state, a more conical, strongly sculptured shell form in the epigean taxa. Although we could not specifically address the selective pressures underlying this morphological parallelism, the fact that a similar kind of morphological divergence was found in the species pair *G. saulae* and *G. filiasaulae* in a different cave in northern Borneo (Haase and Schilthuizen, 2007; Schilthuizen et al., 2012), makes it very likely that a general broadening of the shell, relatively bigger shell size and a reduction in sculpture are a predictable response, at least in hydrocenids, to one or more ecological factors characteristic of the tropical cave environment. As in other environments, these factors may include the abiotic environment (Baur, 1988; Cameron and Cook,

1989; Chiba, 2004; Chiu et al., 2002; Goodfriend, 1986; Haase and Misof, 2009), predation pressure (Moreno-Rueda, 2009; Schilthuizen et al., 2006) and physical restrictions (Okajima and Chiba, 2009).

The maintenance of a distinct morphology in a radically different habitat despite (presumably) gene-flow near the cave entrance, is the hallmark of incipient parapatric species. Under this scenario, the split of the daughter species from only a selection of lineages of the parental species renders the latter paraphyletic (Schilthuizen and Gittenberger, 1996). In a previous paper (Schilthuizen et al., 2005), we followed this reasoning to assign species status to *G. filiasaulae*, and we prefer to do the same here. Therefore, *Georissa* "sp. Silabur" should, in the future, be described as a separate species. (This discovery was made after finalising the taxonomic treatments in Ch. 2 and 3, which is why *Georissa* "sp. Silabur" was not formally described and named yet.)

The non-monophyletic relationship inferred by mitochondrial and nuclear DNA between hydrocenids of Mount Silabur indicates the multiple origins of the hydrocenid fauna here. Both ML and BI topologies (**Figures 4.5 and 4.6**) suggest that typical *G. pyrrhoderma* is sister to *G. sepulutensis* and *G. kinabatanganensis*, *Georissa* "sp. Silabur" is monophyletic, branching off from within the above-ground species *G. pyrrhoderma* (which is thereby rendered paraphyletic), while typical *G. silaburensis* derives from an entirely different ancestral lineage, and is sister to *G. bauensis*. Our ML analyses on separate mitochondrial and nuclear genes show some indications of occasional hybridisation between troglobitic *Georissa* "sp. Silabur" with epigean *G. pyrrhoderma* (see Supporting Information Figures S2 and S3). This is similar to the case of a zone of hybridization between *G. saulae* and *G. filiasaulae* in a cave near Sepulut, Sabah (Schilthuizen et al., 2012). During our sampling, we found only one individual of *Georissa* near the cave entrance, which belongs to the *Georissa* "sp. Silabur" haplotype. So, we suggest that hybridisation between *Georissa* "sp. Silabur" and *G. pyrrhoderma* at Mount Silabur is probably best explained by the rainwater flowing from the upper chambers of the cave to the deep cave habitat.

The haplotype network suggests the hydrocenids of Mount Silabur are clustered based on their shell morphologies, which is in concordance with our

phylogenetic and conchometric analyses. We could not find the shell forms of *G. silaburensis* and *Georissa* "sp. Silabur" in the populations of *G. pyrrhoderma*, or the other way around, despite the variation in shell shape and sculptures of the sympatric species. The similar morphologies in spite of their genetic distinctness between the cave species (*G. silaburensis* and *Georissa* "sp. Silabur") provide evidence for parallelism and cryptic diversity of cave hydrocenids. The cave hydrocenids were collected on the cave walls with continuous slow-flowing water from the cave ceiling which indicates a constant level of moisture, whereas the availability of water or moisture in the external outcrop environment probably fluctuate more strongly. Also, the different food availability of the cave and external outcrop habitats suggest different diet compositions of epigean and hypogean hydrocenids, with green plants available outside, but lacking inside the cave environment. These might be two of many abiotic and biotic factors that lead toward evolving a larger and broader shell morphology in hydrocenids of Mount Silabur.

While it is widely known that rock-dwelling microsnails of Southeast Asia region possess great allopatric divergence in shell shape (for example in the genera *Diplommatina*, *Georissa*, *Gyliotrachela*, *Hungerfordiana*, *Opisthostoma*, and *Plectostoma*; Liew et al., 2014; Rundell, 2008; Schilthuizen et al., 2006; Schilthuizen et al., 2012; Tongkerd et al., 2004; **Chapters 2 and 3**; Yamazaki, Yamazaki, and Ueshima, 2013), our findings provide evidence that morphological convergence may also occur.

Acknowledgement

Authors would like to thank Sarawak Forest Department (SFD) Sarawak and Economic Planning Unit (EPU), Prime Minister Office, Malaysia for the fieldwork permits NCCD.907.4.4(JLD12)-155 (from SFD), UPE40/200/19/3282 (from EPU), export permit: 15982 (from SFD). This study was partially funded by KNAW Ecologie Fond and Treub Foundation awarded to the first author. The first author thanks the Ministry of Education Malaysia for a PhD scholarship award at Naturalis Biodiversity Center and Leiden University, The Netherlands.

References

Aktipis, S. W., and Giribet, G. (2010). A phylogeny of Vetigastropoda and other "archaeogastropods": re-organizing old gastropod clades. *Invertebrate Biology*, 129(3), 220–240.

Alejandrino, A., Puslednik, L., and Serb, J. M. (2011). Convergent and parallel evolution in life habit of the scallops (Bivalvia: Pectinidae). *BMC Evolutionary Biology*, 11(1), 164.

Barr Jr, T. C. (1967). Observations on the ecology of caves. *The American Naturalist*, 101(922), 475–491.

Baur, B. (1988). Microgeographical variation in shell size of the land snail *Chondrina clienta*. *Biological Journal of the Linnean Society*, 35(3), 247–259.

Cameron, R. A. D., and Cook, L. M. (1989). Shell size and shape in Madeiran land snails: do niches remain unfilled? *Biological Journal of the Linnean Society*, 36(1-2), 79–96.

Chazot, N., Panara, S., Zilbermann, N., Blandin, P., Le Poul, Y., Cornette, R., Elias, M., and Debat, V. (2016). Morpho morphometrics: Shared ancestry and selection drive the evolution of wing size and shape in *Morpho* butterflies. *Evolution*, 70(1), 181–194.

Chiba, S. (2004). Ecological and morphological patterns in communities of land snails of the genus Mandarina from the Bonin Islands. *Journal of Evolutionary Biology*, 17(1), 131–143.

Chiu, Y. W., Chen, H. C., Lee, S. C., and Chen, C. A. (2002). Morphometric analysis of shell and operculum variations in the viviparid snail, *Cipangopaludina chinensis* (Mollusca: Gastropoda), in Taiwan. *Zoological Studies*, 41(3), 321–331.

Edgar, R. C. (2004). MUSCLE: multiple sequence alignment with high accuracy and high throughput. *Nucleic acids research*, 32(5), 1792–1797.

Danowitz, M., Vasilyev, A., Kortlandt, V., and Solounias, N. (2015). Fossil evidence and stages of elongation of the *Giraffa camelopardalis* neck. *Royal Society open science*, 2(10), 150393.

Fain, M. G., and Houde, P. (2004). Parallel radiations in the primary clades of birds. *Evolution*, 58(11), 2558–2573.

Folmer, O., Black, M., Hoeh, W., Lutz, R., and Vrijenhoek, R. (1994). DNA primers for amplification of mitochondrial cytochrome c oxidase subunit I from diverse metazoan invertebrates. *Molecular Marine Biology and Biotechnology*, 3(5), 294–299.

Foon, J. K., and Liew, T. S. (2017). A review of the land snail genus *Alycaeus* (Gastropoda, Alycaeidae) in Peninsular Malaysia. *ZooKeys*, 692, 1–81.

Frey, M. A., and Vermeij, G. J. (2008). Molecular phylogenies and historical biogeography of a circumtropical group of gastropods (Genus: Nerita): implications for regional diversity patterns in the marine tropics. *Molecular Phylogenetics and evolution*, 48(3), 1067–1086.

Goodfriend, G. A. (1986). Variation in land-snail shell form and size and its causes: a review. *Systematic Biology*, 35(2), 204–223.

Grenier, J. L., and Greenberg, R. (2005). A biogeographic pattern in sparrow bill morphology: parallel adaptation to tidal marshes. *Evolution*, 59(7), 1588–1595.

Haase, M., and Misof, B. (2009). Dynamic gastropods: stable shell polymorphism despite gene flow in the land snail *Arianta arbustorum*. *Journal of Zoological Systematics and Evolutionary Research*, 47(2), 105–114.

Haase, M., and Schilthuizen, M. (2007). A new *Georissa* (Gastropoda: Neritopsina: Hydrocenidae) from a limestone cave in Malaysian Borneo. *Journal of Molluscan Studies*, 73(3), 215–221.

Hirano, T., Kameda, Y., Kimura, K., and Chiba, S. (2014). Substantial incongruence among the morphology, taxonomy, and molecular phylogeny of the land snails *Aegista*, *Landouria*, *Trishoplita*, and *Pseudobuliminus* (Pulmonata: Bradybaenidae) occurring in East Asia. *Molecular Phylogenetics and Evolution*, 70, 171–181.

Hoang, D. T., Chernomor, O., von Haeseler, A., Minh, B. Q., and Vinh, L. S. (2017). UFBoot2: improving the ultrafast bootstrap approximation. *Molecular Biology and Evolution*, 35(2), 518–522.

Hoekstra, P., and Schilthuizen, M. (2011). Phylogenetic relationships between isolated populations of the limestone-dwelling microsnail *Gyliotrachela hungerfordiana* (Gastropoda: Vertiginidae). *Journal of zoological systematics and evolutionary research*, 49(4), 266–272.

Houle, D. (1992). Comparing evolvability and variability of quantitative traits. *Genetics*, 130(1), 195-204.

Huelsenbeck, J. P., and Ronquist, F. (2001). MRBAYES: Bayesian inference of phylogenetic trees. *Bioinformatics*, 17(8), 754–755.

Hulsey, C. D., Roberts, R. J., Lin, A. S., Guldberg, R., and Streelman, J. T. (2008). Convergence in a mechanically complex phenotype: detecting structural adaptations for crushing in cichlid fish. *Evolution*, 62(7), 1587–1599.

Kaeuffer, R., Peichel, C. L., Bolnick, D. I., and Hendry, A. P. (2012). Parallel and nonparallel aspects of ecological, phenotypic, and genetic divergence across replicate population pairs of lake and stream stickleback. *Evolution*, 66(2), 402–418.

Kalyaanamoorthy, S., Minh, B. Q., Wong, T. K., von Haeseler, A., and Jermiin, L. S. (2017). ModelFinder: fast model selection for accurate phylogenetic estimates. *Nature methods*, 14(6), 587–589.

Khalik, M. Z., Hendriks, K., Vermeulen, J. J., and Schilthuizen, M. (2018). A molecular and conchological dissection of the "scaly" *Georissa* of Malaysian Borneo (Gastropoda, Neritimorpha, Hydrocenidae). *ZooKeys*, 773, 1–51.

Khalik, M. Z., Hendriks, K., Vermeulen, J. J., and Schilthuizen, M. (2019). Conchological and molecular analysis of the "non-scaly" Bornean *Georissa* with the descriptions of three new species (Gastropoda, Neritimorpha, Hydrocenidae). *ZooKeys*, 840, 35–86.

Kumar, S., Stecher, G., and Tamura, K. (2016). MEGA7: molecular evolutionary genetics analysis version 7.0 for bigger datasets. *Molecular biology and evolution*, 33(7), 1870–1874.

Liew, T. S., Vermeulen, J. J., bin Marzuki, M. E., and Schilthuizen, M. (2014). A cybertaxonomic revision of the micro-landsnail genus *Plectostoma* Adam (Mollusca, Caenogastropoda, Diplommatinidae), from Peninsular Malaysia, Sumatra and Indochina. *ZooKeys*, 393, 1–107.

Lindgren, A. R., Pankey, M. S., Hochberg, F. G., and Oakley, T. H. (2012). A multi-gene phylogeny of Cephalopoda supports convergent morphological evolution in association with multiple habitat shifts in the marine environment. *BMC evolutionary biology*, 12(1), 129.

Madsen, O., Scally, M., Douady, C. J., Kao, D. J., DeBry, R. W., Adkins, R., Amrine, H. M., Stanhope, M. J., de Jong W. W., and Springer, M. S. (2001). Parallel adaptive radiations in two major clades of placental mammals. *Nature*, 409(6820), 610–614.

Moreno-Rueda, G. (2009). Disruptive selection by predation offsets stabilizing selection on shell morphology in the land snail *Iberus g. gualtieranus*. *Evolutionary Ecology*, 23(3), 463-471.

Mousseau, T. A., and Roff, D. A. (1987). Natural selection and the heritability of fitness components. *Heredity*, 59(2), 181–197.

Nguyen, L. T., Schmidt, H. A., von Haeseler, A., and Minh, B. Q. (2014). IQ-TREE: a fast and effective stochastic algorithm for estimating maximum-likelihood phylogenies. *Molecular biology and evolution*, 32(1), 268–274.

Okajima, R., and Chiba, S. (2009). Cause of bimodal distribution in the shape of a terrestrial gastropod. *Evolution: International Journal of Organic Evolution*, 63(11), 2877-2887.

Park, J. K., and Ó Foighil, D. (2000). Sphaeriid and corbiculid clams represent separate heterodont bivalve radiations into freshwater environments. *Molecular phylogenetics and evolution*, 14(1), 75–88.

Poulson, T. L., and White, W. B. (1969). The cave environment. *Science*, 165(3897), 971–981.

Price, T. D., Qvarnström, A., and Irwin, D. E. (2003). The role of phenotypic plasticity in driving genetic evolution. *Proceedings of the Royal Society of London. Series B: Biological Sciences*, 270(1523), 1433–1440.

Qi, D., Chao, Y., Guo, S., Zhao, L., Li, T., Wei, F., and Zhao, X. (2012). Convergent, parallel and correlated evolution of trophic morphologies in the subfamily Schizothoracinae from the Qinghai-Tibetan plateau. *PLoS One*, 7, e34070.

Rüber, L., and Adams, D. C. (2001). Evolutionary convergence of body shape and trophic morphology in cichlids from Lake Tanganyika. *Journal of Evolutionary Biology*, 14(2), 325–332.

Revell, L. J., Johnson, M. A., Schulte, J. A., Kolbe, J. J., and Losos, J. B. (2007). A phylogenetic test for adaptive convergence in rock-dwelling lizards. *Evolution*, 61(12), 2898–2912.

Rozas, J., Ferrer-Mata, A., Sánchez-DelBarrio, J. C., Guirao-Rico, S., Librado, P., Ramos-Onsins, S. E., and Sánchez-Gracia, A. (2017). DnaSP 6: DNA sequence polymorphism analysis of large data sets. *Molecular Biology and Evolution*, 34(12), 3299–3302.

Rundell, R. J. (2008). Cryptic diversity, molecular phylogeny and biogeography of the rock- and leaf litter-dwelling land snails of Belau (Republic of Palau, Oceania). *Philosophical Transactions of the Royal Society B: Biological Sciences*, 363(1508), 3401–3412.

Rundle, H. D., and Nosil, P. (2005). Ecological speciation. *Ecology letters*, 8(3), 336-352.

RStudio Team (2016). RStudio: Integrated Development for R. RStudio, Inc., Boston, MA. URL: http://www.rstudio.com/

Schilthuizen, M., Cabanban, A. S., and Haase, M. (2005). Possible speciation with gene flow in tropical cave snails. *Journal of Zoological Systematics and Evolutionary Research*, 43(2), 133–138.

Schilthuizen, M., and Gittenberger, E. (1996). Allozyme variation in some Cretan *Albinaria* (Gastropoda): paraphyletic species as natural phenomena. In: Taylor J. D. (Ed.) Origin and Evolutionary Radiation of the Mollusca. Oxford University Press Inc., New York, 301–311.

Schilthuizen, M., Rutten, E. M., and Haase, M. (2012). Small-scale genetic structuring in a tropical cave snail and admixture with its above-ground sister species. *Biological Journal of the Linnean Society*, 105(4), 727–740.

Schilthuizen, M., Til, A. V., Salverda, M., Liew, T. S., James, S. S., Elahan, B. B., and Vermeulen, J. J. (2006). Microgeographic evolution of snail shell shape and predator behavior. *Evolution*, 60(9), 1851–1858.

Schluter, D. (2009). Evidence for ecological speciation and its alternative. *Science*, 323(5915), 737–741.

Stayton, C. T. (2006). Testing hypotheses of convergence with multivariate data: morphological and functional convergence among herbivorous lizards. *Evolution*, 60(4), 824–841.

Thompson, F. G., and Dance, S. P. (1983). Non-marine Mollusks of Borneo: II Pulmonata: Pupillidae, Clausiliidae: III Prosobranchia: Hydrocenidae, Helicinidae. *Bulletin of the Florida State Museum Biological Sciences*, 29(3), 101–152.

Tongkerd, P., Lee, T., Panha, S., Burch, J. B., and Ó Foighil, D. (2004). Molecular phylogeny of certain Thai gastrocoptine micro land snails (Stylommatophora: Pupillidae) inferred from mitochondrial and nuclear ribosomal DNA sequences. *Journal of Molluscan Studies*, 70(2), 139–147.

Vermeulen, J. J., Liew, T. S., and Schilthuizen, M. (2015). Additions to the knowledge of the land snails of Sabah (Malaysia, Borneo), including 48 new species. *ZooKeys*, 531, 1–139.

Via, S. (2009). Natural selection in action during speciation. *Proceedings of the National Academy of Sciences*, 106, 9939–9946.

Wilford, G. E. (1964). The geology of Sarawak and Sabah caves (No. 6): Geological Survey, Borneo Region, Malaysia. Brunei Press Limited, Brunei.

Yamazaki, K., Yamazaki, M., and Ueshima, R. (2013). Systematic review of diplommatinid land snails (Caenogastropoda, Diplommatinidae) endemic to the Palau Islands. (1) Generic classification and revision of *Hungerfordia* species with highly developed axial ribs. *Zootaxa*, 3743(1), 1–71.

Supplementary materials

Link to supplementary materials1-9
https://onlinelibrary.wiley.com/action/downloadSupplement?doi=10.1111%2Fjzs.12352andfile=jzs12352-sup-0001-Supinfo.pdf

1. **Table S1** Shell measurement of all hydrocenids used in Principal Component Analysis (PCA) and their shell form.
2. **Table S2** List of specimens used in molecular analyses and their GenBank accession number.
3. **Table S3** Haplotype group of each individuals based on partial *COI* mtDNA.
4. **Figure S1a** Plots of AW vs. SH of different hydrocenid shell forms at Mount Silabur.
5. **Figure S1b** Plots of AW vs. SH of different shell forms at Mount Silabur.
6. **Figure S1c** Plots of AH vs. SW of different shell forms at Mount Silabur.
7. **Figure S1d** Plots of AW vs. SW of different shell forms at Mount Silabur.
8. **Figure S2** Maximum likelihood tree inferred by concatenated partial *16S* and *CO1* mtDNA.
9. **Figure S3** Maximum likelihood tree inferred by *28S* nDNA.
10. **Sequence alignment A1** *16S* sequence alignment.
https://onlinelibrary.wiley.com/action/downloadSupplement?doi=10.1111%2Fjzs.12352andfile=jzs12352-sup-0002-AlignmentA1.fasta
11. **Sequence alignment A2** *28S* sequence alignment.
https://onlinelibrary.wiley.com/action/downloadSupplement?doi=10.1111%2Fjzs.12352andfile=jzs12352-sup-0003-AlignmentA2.fasta
12. **Sequence alignment A3** *COI* sequence alignment.
https://onlinelibrary.wiley.com/action/downloadSupplement?doi=10.1111%2Fjzs.12352andfile=jzs12352-sup-0004-AlignmentA3.fasta